The Astrophysical Journal Letters, 840:L8 (7pp), 2017 May 1 https://doi.org/10.3847/2041-8213/aa6d56


# Alternative Energy: Production of $H_2$ by Radiolysis of Water in the Rocky Cores of Icy Bodies

Alexis Bouquet[1,2], Christopher R. Glein[2], Danielle Wyrick[2], and J. Hunter Waite[1,2]
[1] Department of Physics and Astronomy, University of Texas at San Antonio, San Antonio, TX, USA
[2] Southwest Research Institute, Space Science and Engineering Division, San Antonio, TX, USA
*Received 2017 February 17; revised 2017 April 8; accepted 2017 April 12; published 2017 April 27*

## Abstract

We applied a model of radiolysis in earthly rock–water mixtures to several known or suspected ocean worlds: Enceladus, Ceres, Europa, Titania, Oberon, Pluto, and Charon. In this model, radiation emitted by the long-lived radionuclides ($^{40}$K, $^{232}$Th, $^{235}$U, and $^{238}$U) contained in the ordinary chondrite-like rocks is partly absorbed by the water permeating the material of each body's core. The physical and chemical processes that follow release molecular hydrogen ($H_2$), which is a molecule of astrobiological interest. We compared the calculated production of $H_2$ by radiolysis in each body's core to published estimates of production by serpentinization. This study presents production calculations over 4.5 Gyr for several values of rock porosity. We found that radiolysis can produce $H_2$ quantities equivalent to a few percent of what is estimated from serpentinization. Higher porosity, which is unlikely at the scale of a body's entire core but possible just under the seafloor, can increase radiolytic production by almost an order of magnitude. The products of water radiolysis also include several oxidants, allowing for production of life-sustaining sulfates. Though previously unrecognized in this capacity, radiolysis in an ocean world's outer core could be a fundamental agent in generating the chemical energy that could support life.

*Key words:* astrobiology – planets and satellites: interiors – planets and satellites: oceans

## 1. Introduction

Molecular hydrogen ($H_2$) is a major product of water radiolysis, along with $H_2O_2$ and OH. Its production rates have been studied out of concern for safety in nuclear waste storage (Le Caër 2011) and as a potential source of chemical energy for underground biotic systems on Earth (e.g., Lin et al. 2005a, 2005b, 2006; Blair et al. 2007). Microbial communities sustained by $H_2$ have been found on Earth (Pedersen 2000; D'hondt et al. 2004), raising interesting possibilities for astrobiology and the potential existence of analogous communities at the water–rock interface of ocean worlds such as Enceladus or Europa.

The most frequently considered source of $H_2$ on ocean worlds is high-temperature hydrothermalism (McCollom 1999; Hand et al. 2007). More recently, serpentinization has gained attention in the field of astrobiology (Vance et al. 2016) due to its potential to produce $H_2$ and heat and the parallel with observed ecosystems on Earth, such as Lost City (Kelley et al. 2001), and the accessibility of smaller body cores to water. However, serpentinization relies on the exposure of unreacted materials to maintain its production and does not generate oxidants.

In any rock penetrated by water (as assumed for serpentinization to occur), the decay of long-lived radionuclides would expose water to $\alpha$, $\beta$, and $\gamma$ radiation (see Figure 1). Final products of this process include $H_2$. Once a section of the core is exposed to water, radiolysis ensures a steady $H_2$ production in this section, independently of the future evolution (or lack thereof) of the serpentinization front.

This study estimates $H_2$ production by water radiolysis in the cores of several bodies known to or likely to host liquid water oceans, analyzing its importance relative to serpentinization. We started from the results of Vance et al. (2016) and followed their scenario of water accessing the rocky core deeper and deeper with time. We used the model of Hofmann (1992) to calculate the production of $H_2$ over time for the part of the core exposed to water and compared this estimate with the result of Vance et al. (2016) for serpentinization.

The potential $H_2$ production by radiolysis has already been quantified for Earth (e.g., Lin et al. 2005a) and is being studied for Mars (Tarnas et al. 2017). We focused on icy bodies known to or suspected to host a subsurface liquid water ocean: Enceladus, Europa, Ceres, Titania, Oberon, Pluto, and Charon. Our analysis used bodies studied in Vance et al. (2016) to directly compare $H_2$ production. Spacecraft data have shown the existence of oceans on Enceladus and Europa (Khurana et al. 1998; Postberg et al. 2009; Iess et al. 2014; Thomas et al. 2016), and their geyser activity (Porco et al. 2006; Roth et al. 2014; Sparks et al. 2016) allows indirect sampling of their oceans, facilitating the study of their astrobiological potential. Ceres may also host an ocean according to models of its evolution, depending on the scenario considered (Neumann et al. 2015; Neveu et al. 2015) and the amount of $NH_3$ in the water; *Dawn* measurements indicate a substantial presence of ammonia (De Sanctis et al. 2015). Ceres also presents the interesting characteristic of its "intermediate" size compared to the other bodies of the list: bigger than Enceladus, but smaller than Titania/Oberon. Pluto, with its relatively large radius but presumably thin serpentinized layer, offers a unique case. Its satellite Charon is itself intermediate between Ceres and Titania/Oberon.

In Section 2, we explain the required inputs for the model and our geophysical assumptions. In Section 3, we provide the results of the computations and compare them to serpentinization estimates by Vance et al. (2016). We discuss the implications and the possible variations introduced by our assumptions in Section 4.

## 2. Model of Radiolysis in Rocky Cores

### *2.1. Calculation of $H_2$ Production*

To estimate the amount of $H_2$ produced, we used the radiolysis model cited in Hofmann (1992), originally from

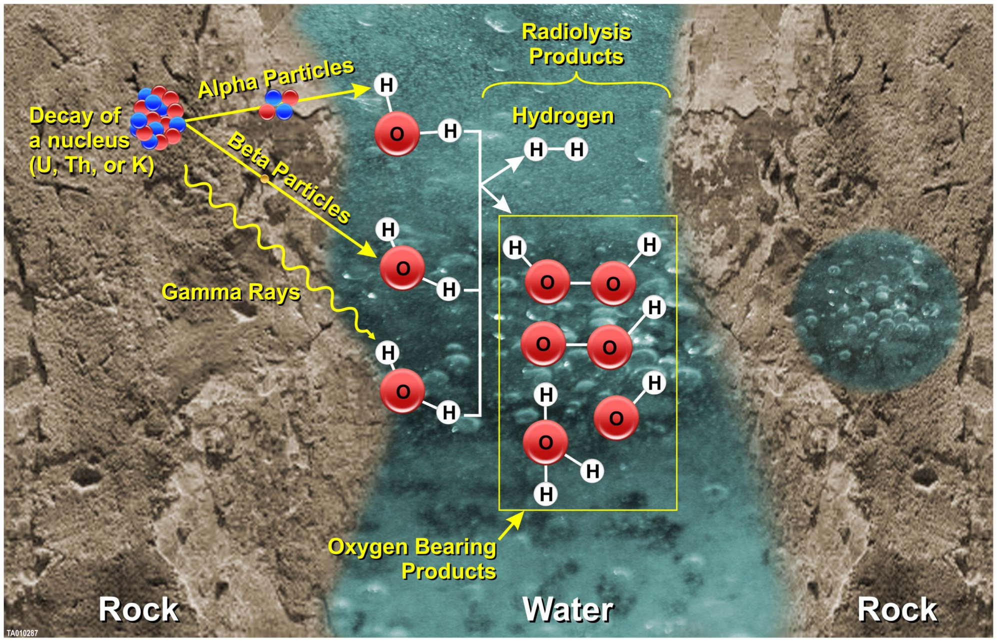


**Figure 1.** Summary of the process of water radiolysis by radionuclides. The radiolysis products are the result of several physico-chemical steps that follow the excitation/ionization of water by radiation. The full chain of reactions and the exhaustive list of products can be found in Le Caër (2011).

Aitken (1985), which has been similarly used for Earth (Lin et al. 2005a).

The total quantity of $H_2$ produced in a volume $V$ of rock–water material per unit of time is

$$P_{H_2} = \sum_i (G_{H_2,i} \sum_s D_{s,i}), \tag{1}$$

where $s$ is a type of radionuclide (e.g., $^{232}$Th), $i$ a type of emission (e.g., $\alpha$ particles), $G_{H_2,i}$ is the radiation chemical yield of $H_2$ in water for radiation type $i$, and $D_{s,i}$ is the radiation dose absorbed by water due to radiation type $i$ emitted by radionuclide $s$. We used the following values of yield: $G_{H_2,\alpha} = 0.96$, $G_{H_2,\beta} = 0.6$, $G_{H_2,\gamma} = 0.4$, all in molecules/100 eV (Harris & Pimblott 2002; Lin et al. 2005b).

$D_{s,i}$ is given by an equation from Hofmann (1992) that we modified to include porosity:

$$D_{s,i} = \frac{V\rho_r A_s \sum E_{i,s}}{\frac{1}{1-\phi} + \frac{\rho_r}{S_i \rho_w \phi}}, \tag{2}$$

where $\rho_r$ is the grain density, $\rho_w$ is the water density, $A_s$ is the activity of species $s$ (decays per unit of time per unit of mass of rock), $\sum E_{i,s}$ is the energy decay sum for species $s$ emitted as radiation type $i$, $\phi$ is the porosity, and $S_i$ is the ratio of mass stopping powers of water to rock, with values of $S_\alpha = 1.5$, $S_\beta = 1.25$, $S_\gamma = 1.14$ (Hofmann 1992). The $\sum E_{i,s}$ values we used are detailed in Table 1. We use $\rho_r = 3.0$ g cm$^{-3}$ for hydrated chondrite rock, as calculated in Waite et al. (2017) for Enceladus. Depending on the body, $\rho_r$ values may differ; Equation (2) implies the total production varies linearly with rock density. For example, a range of densities from 2.5 to 3.5 g cm$^{-3}$ amounts to a 17% decrease/increase of the values presented in our work. Derivation of Equation (2) is provided in the Appendix.

We included activity from four long-lived radionuclides: $^{40}$K, $^{232}$Th, $^{235}$U, and $^{238}$U. To facilitate comparisons, we used the chondritic abundances of Vance et al. (2016) and deduced $^{40}$K and $^{235}$U by using the ratios of Lodders (2003). The abundances are summarized in Table 1.

The remaining input parameter, porosity, is discussed in Section 2.2.

### 2.2. Porosity

Porosity is the interstitial void space present in a given volume of rock and is created by different types of interstices, including fractures. If this interstitial space is filled with water, the porosity value, equivalent to the ratio of the volume of water to the combined volume of rock and water, sets the rate of radiolysis.

Chondrites can feature porosities as high as 30%; however, the cores of bodies the size of Ceres or larger can be expected to be transformed by multiple factors during their evolution. Neumann et al. (2015) show for Ceres that creep reduces porosity in the core to almost zero in a few hundred Myr. Updating their calculations to account for liquid water (Neumann et al. 2016a) leaves only a thin layer below the seafloor (∼1–2 km) still featuring porosity of a few percent (Neumann et al. 2016b).

Permeability, the capacity of rock to transmit a fluid through fractures and/or pores (porous flow, as in sandstones), determines whether the volume is accessible to water in the first place. Chondrites show a low permeability due to the fine grain size of the materials (Bland et al. 2009). The model used in Vance et al. (2007, 2016) lets water infiltrate the core as cooling-induced thermal cracking enhances permeability. Vance et al. (2016) assume serpentinization impacts the whole outer core and that all the fayalite (10% of the olivine) is processed into magnetite. Their estimate can be considered an upper limit for the production; the serpentinization may occur only in a part of the volume considered if the fracture connectivity is not extensive (Sim & Kim 2005), and ferrous serpentine production may occur, which

**Table 1**
Concentration of Radionuclides Used for the Model, Half-lives, and Energy Imparted by Decay Sequence for Each Type of Radiation

| | Concentration in Ordinary Chondrites (ppb)[a,b] | Half-life (years) | $\alpha$ Decay Energy Sum[c] (MeV/decay) | $\beta$ Decay Energy Sum[c] (MeV/decay) | $\gamma$ Decay Energy Sum[c] (MeV/decay) |
|---|---|---|---|---|---|
| $^{40}$K | 105 | $1.25 \times 10^9$ | 0 | 1.1760 | 0.1566 |
| $^{232}$Th | 40 | $1.4 \times 10^{10}$ | 35.95 | 2.8408 | 2.2447 |
| $^{235}$U | 0.087 | $7.04 \times 10^8$ | 34.03 | 10.4470 | 0.55 |
| $^{238}$U | 12 | $4.46 \times 10^9$ | 42.97 | 6.0935 | 1.7034 |

**Notes.**
[a] Vance et al. (2016).
[b] Lodders (2003).
[c] Blair et al. (2007).

would not generate $H_2$. We considered radiolysis throughout the whole serpentinized volume. Even if water cannot access the whole core, the ratio of the productions we obtain is an indication of the relative contribution of radiolysis compared to serpentinization. For serpentinization production it is assumed that transformation of the rock is instant at geological timescales. The temperatures at the serpentinization front calculated by Vance et al. (2016) are over 50°C at the present epoch in all bodies except Pluto. Experiments show at least 0.01% of the exposed material is converted per day (McCollom et al. 2016). The rates are comparable over the explored range of temperatures: 50°C and above (Mayhew et al. 2013). The timescale of serpentinization of material exposed to water is probably counted in days in ocean worlds, while the serpentinization front progresses at most at 22 $\mu$m yr$^{-1}$ in the case of Charon. The assumption of immediate serpentinization at the geological timescale can be taken as an endmember approximation.

Experiments on serpentinized rocks from Earth's seafloor show a porosity of 2%–3% and a high permeability (Macdonald & Fyfe 1985). We adopted these values as our lower boundary: 2.5% porosity and homogeneous in the serpentinized volume.

As an upper boundary, we used a profile based on the most porous material from Zolotov (2009) for each body. These values are based on an empirical relationship derived from earthly sediments. In this model, the porosity $\phi$ is calculated with

$$\phi = \phi_0 \exp(-ch) = \phi_0 \exp\left(\frac{-cP}{\rho_e g_e}\right), \tag{3}$$

where $\phi_0$ is the porosity at a pressure of 0 Pa ($\phi_0 = 0.55$, from Figure 2 of Zolotov 2009), $c$ is a constant depending on the type of rock (0.27, typical for sandstones, is used to find an upper bound to our estimates), $h$ is the depth into the rock, $P$ is the pressure at depth $h$, $\rho_e$ is the density of materials considered in the original formula (2700 kg m$^{-3}$), and $g_e$ is Earth's surface gravity acceleration (9.81 m s$^{-2}$). Equation (3) gives a porosity profile as a function of any body's pressure profile (itself a function of its gravity profile and the density of its materials).

Owing to the way Vance et al. (2016) calculated Enceladus's serpentinization production (constant production, by averaging the full serpentinization of the core over the age of Enceladus), we separate our results for Enceladus from the other bodies to avoid misleading comparisons. As with the other bodies, we consider a minimum porosity of 2.5% for the whole core. However, since the lower-gravity environment of Enceladus allows for high porosities in the core, we include a case for 30% homogeneous porosity (Roberts 2015).

## 3. Results

We calculated of $H_2$ production by radiolysis for each of the bodies considered, from 4.5 billions years ago to the present day. We used the calculation results of Vance et al. (2016) for the progression of the serpentinization front with time; only the serpentinized portion of the core participates in the production of $H_2$.

For each case, we plot the ratio of yearly production by radiolysis to the yearly production by serpentinization (as estimated in Vance et al. 2016), the yearly $H_2$ production by radiolysis, the integrated $H_2$ production by radiolysis, and the ratio of integrated productions (radiolysis versus serpentinization).

Figure 2 shows general results on the production of $H_2$ as a function of porosity, and Figure 3 displays calculation results for all bodies except Enceladus, shown in Figure 4.

From these calculations, the following results apply to all bodies considered:

1. For the range of values considered in this study, a higher porosity translates into a higher $H_2$ production (Figure 2(a)). As porosity decreases, so does the total $H_2$ production of a given volume of rock–water material, but the amount of energy deposited per unit of volume of water increases. This is due to a larger volume of rock emitting more total energy. The local concentration $H_2$ can reach in water, assuming no escape, varies by only ~5% (Figure 2(b)) in the 0.1%–10% porosity range.
2. Yearly production by radiolysis decreases with time. While the serpentinization front progresses and a larger fraction of the core is exposed to water, thus participating in radiolysis, the reduction in radionuclide abundances more than compensates for this. This is true over the whole range of sizes and rates of evolution considered here.
3. For each body, the relative importance of radiolysis first declines as radionuclide abundances decrease while serpentinization occurs in the outermost layers of the core, where the most material is readily available. Later (−1.5 to −1.0 Gyr), the relative importance of radiolysis rises again as serpentinization slows down when deeper layers are reached.
4. The ratio of accumulated productions of $H_2$ by radiolysis versus serpentinization decreases with time, seemingly converging asymptotically toward a value specific to the body considered.
5. Porosity strongly influences the relative importance of serpentinization to radiolysis, as illustrated by the differences between Figures 3(a) and (b), as well as within Figure 4. In the cases that consider the highest porosities,

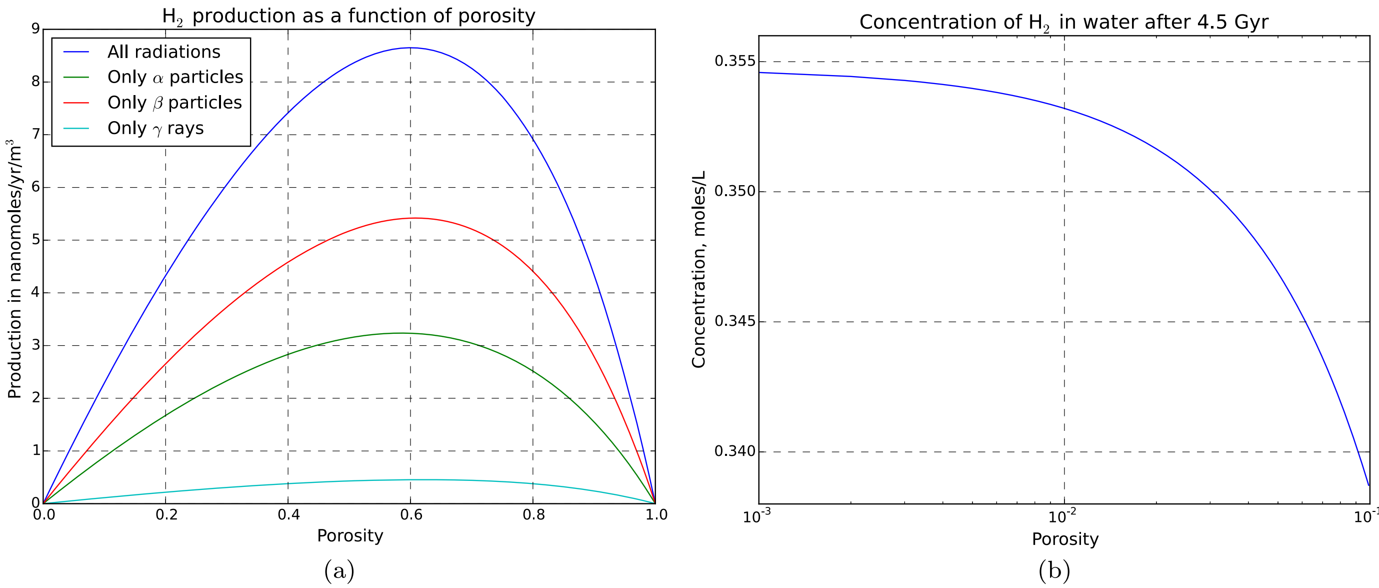


**Figure 2.** (a) Dependence of $H_2$ production on porosity in 1 $m^3$ of material. We show the total production and the separate contributions of each type of radiation. (b) Concentration of $H_2$ achieved after 4.5 Gyr, as a function of porosity.

the accumulated production by radiolysis can reach a significant fraction of the production by serpentinization: more than 25% for Ceres (Figure 3(b)), more than 30% for Enceladus (Figure 4).

The more important production of Ceres or Charon relative to Titania or Oberon (for example) shows that bigger bodies may not necessarily have the best potential for habitability.

## 4. Discussion

Our results show that production of $H_2$ by radiolysis can reach values that make it relevant to astrobiology. This production can be from a few percent to almost one-third of the estimated production by serpentinization over the life of an ocean world. Radiolysis is inevitable once water is exposed to radionuclide-bearing materials, in contrast with serpentinization that requires exposing new, unreacted material. The most influential parameter in our study for production per unit of volume, and the most unconstrained, is the porosity of rocky cores. While thermal cracking and pore expansion (Neveu et al. 2015; Vance et al. 2016) can favor the circulation of water in the core, other processes such as creep (Neumann et al. 2015, 2016a) could compact the core to the point that only a thin external layer (1–2 km) would be porous and accessible to water (Neumann et al. 2016b). Examples on Earth show the production per unit volume can still be sufficient to maintain microbial communities (Lin et al. 2005b).

As modeling of ocean world cores progresses, our assessment of $H_2$ production will evolve. In particular, the history of Enceladus can lead to different conclusions. For instance, the ocean could be recent, e.g., due to a late formation of Enceladus (Ćuk et al. 2016); therefore, serpentinization would still be occurring in the outer layers of the core and its production would by far exceed radiolysis. If the ocean is old and the core is fully serpentinized (Vance et al. 2016), radiolysis could be the only $H_2$ source left today.

Radiolysis needs to be considered in the redox budget of the subsurface. Oxidants such as OH and $H_2O_2$ (Le Caër 2011) are likely to oxidize surrounding reduced materials, e.g., to form sulfates where in contact with sulfide minerals like pyrrhotite (Li et al. 2016). This production can be compared with oxidants from other sources such as surface radiolysis. In the case of Europa, the yearly $O_2$ flux from the surface is estimated between $3.10^8$ and $3.10^{11}$ moles $yr^{-1}$ (Hand et al. 2007; Greenberg 2010). Our estimates of production of $H_2$ fall within that range, from 0.4 to $1.10^9$ moles $yr^{-1}$ (Figure 3). For Enceladus the maximum production of $O_2$ by radiolysis on the surface, unlikely to reach the ocean in its entirety as only part of the surface is active, is estimated at $5.10^7$ moles $yr^{-1}$ (Waite et al. 2017). Our results indicate current $H_2$ production up to $1.10^8$ moles $yr^{-1}$ (Figure 4). These two cases indicate a potentially significant contribution of endogenic radiolysis to the redox budget.

The previously mentioned production of sulfate could allow for another commonly discussed life-sustaining reaction: sulfur reduction (Gaidos et al. 1999). Therefore, radiolysis can sustain biogenic activity in more than one way.

The production of oxidants by radiolysis has implications for the chemical evolution of chondrites (Cody & Alexander 2005), especially shortly after CAIs when short-lived isotopes would have made a significant contribution.

One important caveat is that the model assumes homogeneous spatial deposition of radiation energy. If rock pebble size is not significantly smaller than the range of emitted particles, $\alpha$ and $\beta$ radiation contribution would be mitigated or suppressed (Dzaugis et al. 2015), depending on the exact scale of irregularities. Figure 2(a) allows a rough quantification of this effect depending on the mitigation of each particle type.

Radiolysis may have been influential in comet interiors. Water-ice radiolysis forms volatiles including $H_2$ and $O_2$ (Zheng et al. 2006). The ice-to-rock volume ratio of a comet would likely be closer to the optimum for radiolytic production seen in Figure 2(a), but yields in ice are lower since the ice matrix hinders diffusion of the products, favoring recombination into water (Spinks & Woods 1990).

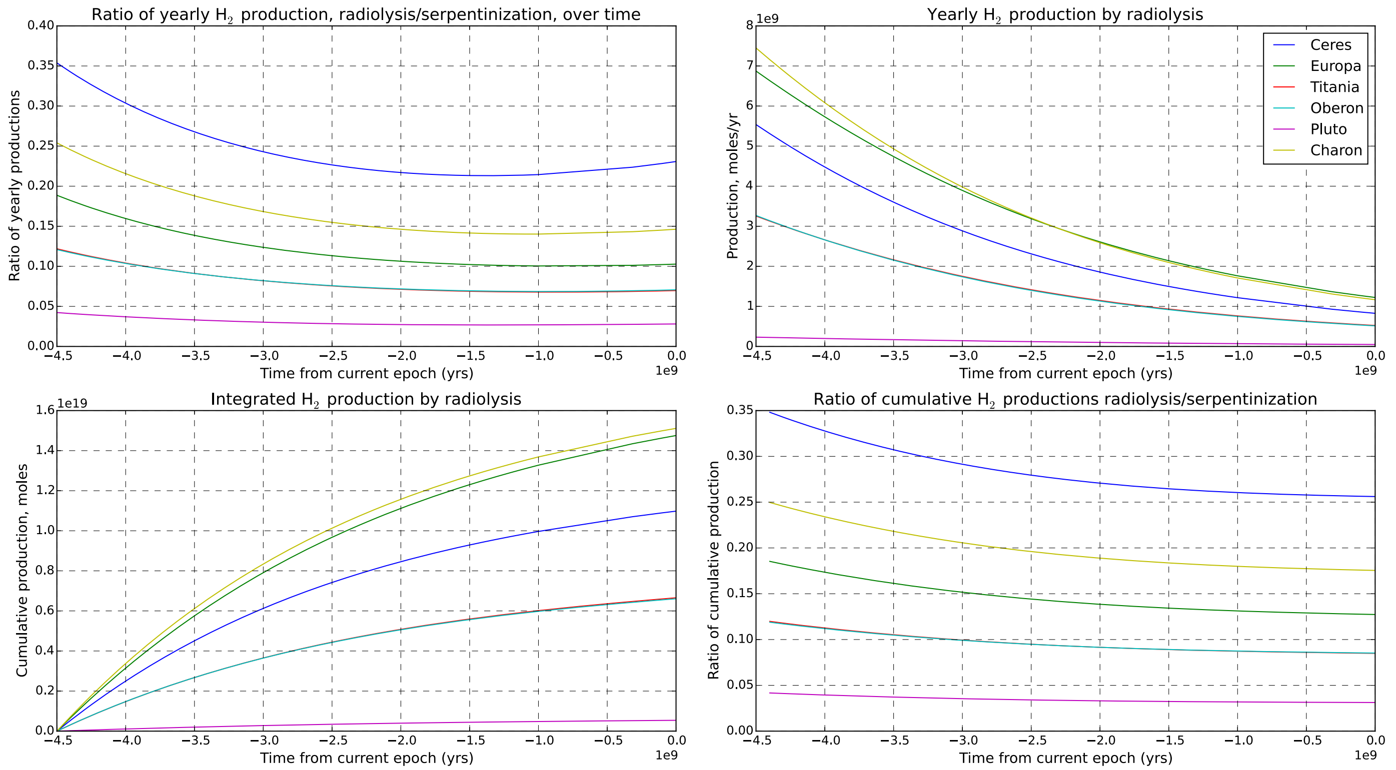


(a)

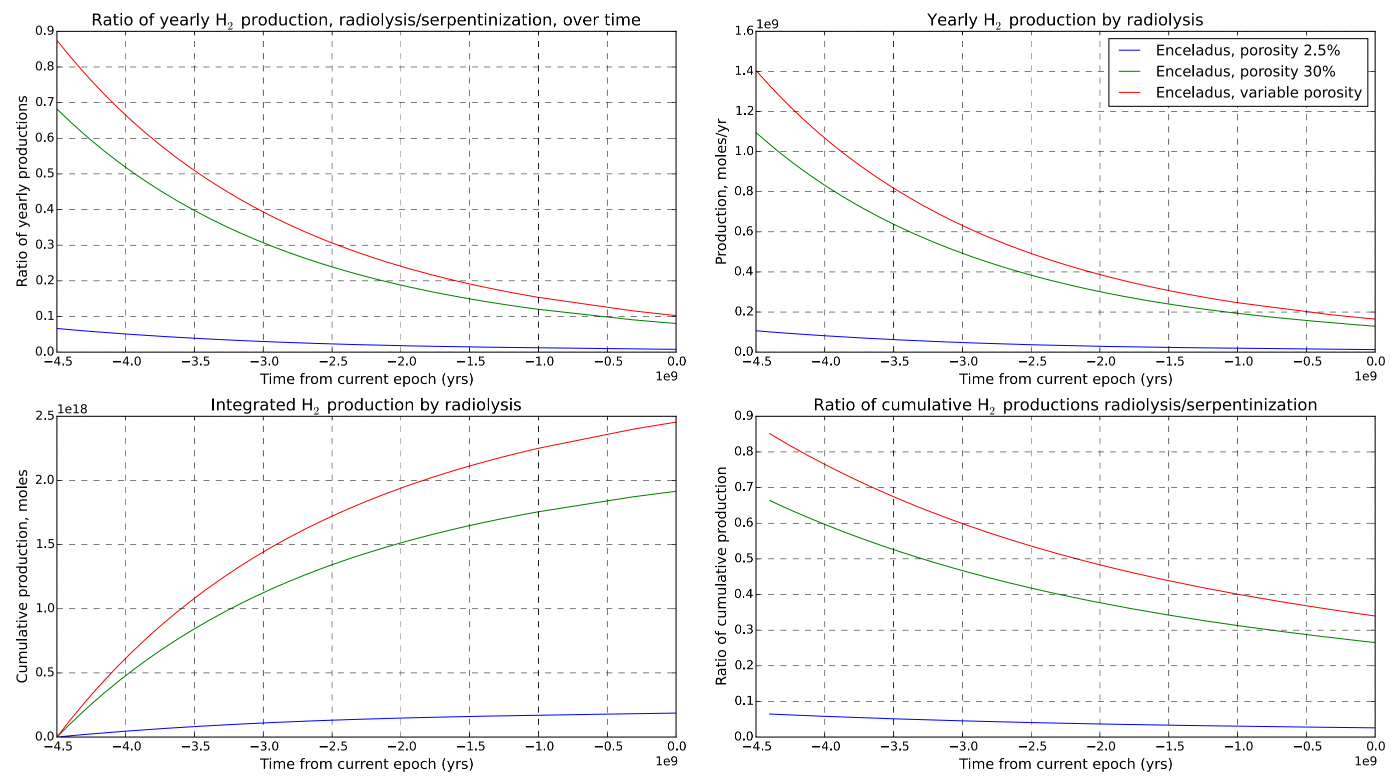


(b)

**Figure 3.** (a) All bodies, 2.5% homogeneous porosity. (b) All bodies, porosity profile following Equation (3), as per Zolotov (2009). Values for sandstone are used to provide an upper boundary to the problem. Serpentinization production and percolation depth are from Vance et al. (2007, 2016).

An observational indication of extensive transformation by radiolysis would be a characteristic $H_2/^4He$ ratio in water (Sherwood Lollar et al. 2014). Irradiation by $\alpha$ particles effectively adds $^4He$ nuclei directly into water, while other $H_2$ sources do not. Another indicator would be the presence of sulfates on bodies where it cannot be attributed to surface radiolysis.

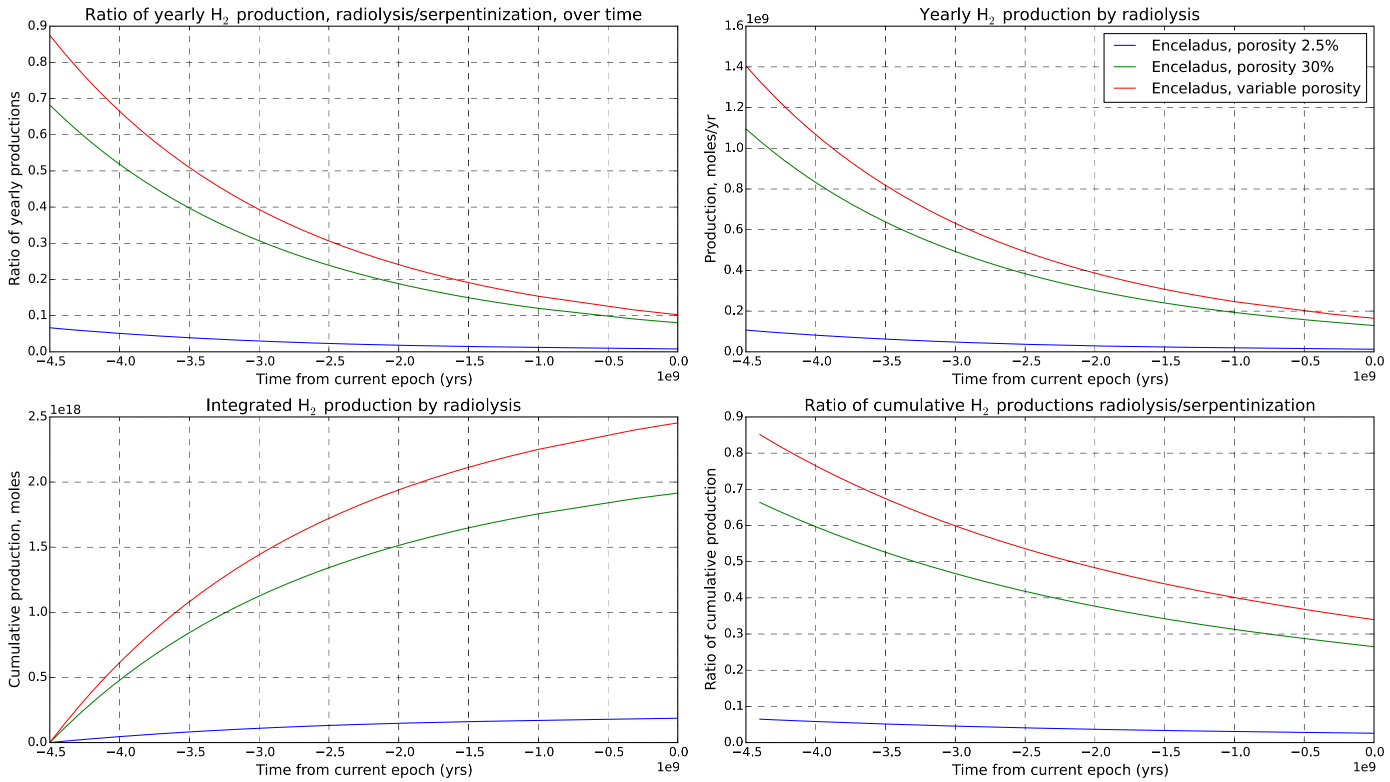


**Figure 4.** Comparison of Enceladus with 2.5% and 30% homogeneous porosity, and a porosity profile following Equation (3), as per Zolotov (2009). The serpentinization production used for comparison, as per Vance et al. (2016), is constant (serpentinization of the whole core over 4.5 Gyr).

The Earth is hypothesized to host a massive intraterrestrial biosphere, partly driven by molecular hydrogen (Pedersen 2000). Radiolysis could create habitable conditions in other bodies of the solar system by producing $H_2$ and oxidants. While serpentinization is a more efficient source of $H_2$, it is dependent on the continuous exposure of unreacted rock and appropriate temperature conditions. Radiolysis can potentially sustain microbial communities where serpentinization has stopped or where its products are not available. Understanding the contribution of radiolytic $H_2$ expands the range of icy bodies potentially capable of significant $H_2$ production, and thus of sustaining a chemical disequilibrium favorable to habitability.

Plots drawn with Matplotlib (Hunter 2007). This work is supported by the Cassini Project through JPL subcontract 1405853 and by the Rosina project through JPL subcontract 1296001. We thank Steve Vance for sending us the results of his simulations and for fruitful discussions.

## Appendix
## Calculation of the Energy Deposited in Water

$D_{s,i}$ as defined in Section 2 is given by (Hofmann 1992)

$$D_{s,i} = \frac{D_{es,i} W S_i}{1 + W S_i}, \tag{4}$$

where $D_{es,i}$ is the energy emitted in the considered volume by radionuclide $s$ through radiation type $i$, $W$ is the weight ratio of water to rock, and $S_i$ is the ratio of mass stopping powers of water to rock.

Using the subscript $w$ for quantities related to water and $r$ for quantities related to rock, we expand $W$ as

$$W = \frac{\rho_w V_w}{\rho_r V_r}, \tag{5}$$

where $\rho_w$ and $\rho_r$ are the densities of water and rock, respectively, and $V_w$ and $V_r$ the volume they occupy, the total volume being $V = V_r + V_w$.

Equation (4) then becomes

$$D_{s,i} = \frac{D_{es,i} \rho_w V_w / (\rho_r V_r) S_i}{1 + \rho_w V_w / (\rho_r V_r) S_i} = \frac{D_{es,i}}{1 + \rho_r V_r / (\rho_w V_w S_i)}. \tag{6}$$

By introducing the porosity $\phi$,

$$\phi = \frac{V_w}{V_r + V_w}; \tag{7}$$

we can now rewrite $V_w$ and $V_r$ as

$$V_w = \phi (V_r + V_w), \tag{8}$$

$$V_r = (1 - \phi)(V_r + V_w). \tag{9}$$

Therefore,

$$D_{s,i} = \frac{D_{es,i}}{1 + \frac{\rho_r}{\rho_w S_i} \frac{V_r}{(V_r + V_w)\phi}} = \frac{D_{es,i}}{1 + \frac{\rho_r}{\rho_w S_i} \frac{1 - \phi}{\phi}}. \tag{10}$$

We also expand $D_{es,i}$ as

$$D_{es,i} = V_r \rho_r A_s \sum E_{i,s}, \tag{11}$$

where $A_s$ is the activity of species $s$ (decays $s^{-1}$ $kg^{-1}$), deduced from its abundance, decay constant, and atomic mass (Table 1).

By using Equation (9) to replace $V_r$ in Equation (11), we can rewrite Equation (10) as

$$D_{s,i} = \frac{(1-\phi)(V_r + V_w)\rho_r A_s \sum E_{i,s}}{1 + \frac{\rho_r}{\rho_w S_i}\frac{1-\phi}{\phi}} = \frac{V\rho_r A_s \sum E_{i,s}}{\frac{1}{1-\phi} + \frac{1}{S'_i \phi}}, \quad (12)$$

where $S_i' = S_i \rho_w/\rho_r$.

## References


Aitken, M. J. 1985, Thermoluminescence Dating (New York: Academic)
Blair, C. C., D'Hondt, S., Spivack, A. J., & Kingsley, R. H. 2007, AsBio, 7, 951
Bland, P. A., Jackson, M. D., Coker, R. F., et al. 2009, E&PSL, 287, 559
Cody, G. D., & Alexander, C. M. 2005, GeCoA, 69, 1085
Ćuk, M., Dones, L., & Nesvorný, D. 2016, ApJ, 820, 97
D'hondt, S., Jørgensen, B. B., Miller, D. J., et al. 2004, Sci, 306, 2216
De Sanctis, M., Ammannito, E., Raponi, A., et al. 2015, Natur, 528, 241
Dzaugis, M. E., Spivack, A. J., & D'Hondt, S. 2015, RaPC, 115, 127
Gaidos, E. J., Nealson, K. H., & Kirschvink, J. L. 1999, Sci, 284, 1631
Greenberg, R. 2010, AsBio, 10, 275
Hand, K. P., Carlson, R. W., & Chyba, C. F. 2007, AsBio, 7, 1006
Harris, R. E., & Pimblott, S. M. 2002, Radiation Research, 158, 493
Hofmann, B. 1992, in Proc. 7th Int. Symp. on Water-Rock Interaction, ed. Y. K. Kharaka & A. S. Maest (Rotterdam: Balkema), 503
Hunter, J. D. 2007, CSE, 9, 90
Iess, L., Stevenson, D., Parisi, M., et al. 2014, Sci, 344, 78
Kelley, D. S., Karson, J. A., Blackman, D. K., et al. 2001, Natur, 412, 145
Khurana, K., Kivelson, M., Stevenson, D., et al. 1998, Natur, 395, 777
Le Caër, S. 2011, Water, 3, 235
Li, L., Wing, B., Bui, T., et al. 2016, NatCo, 7, 13252
Lin, L.-H., Hall, J., Lippmann-Pipke, J., et al. 2005a, GGG, 6, Q07003
Lin, L.-H., Slater, G. F., Lollar, B. S., Lacrampe-Couloume, G., & Onstott, T. 2005b, GeCoA, 69, 893
Lin, L.-H., Wang, P.-L., Rumble, D., et al. 2006, Sci, 314, 479
Lodders, K. 2003, ApJ, 591, 1220
Macdonald, A., & Fyfe, W. 1985, Tectp, 116, 123
Mayhew, L., Ellison, E., McCollom, T., Trainor, T., & Templeton, A. 2013, NatGe, 6, 478
McCollom, T. M. 1999, JGR, 104, 30729
McCollom, T. M., Klein, F., Robbins, M., et al. 2016, GeCoA, 181, 175
Neumann, W., Breuer, D., & Spohn, T. 2015, A&A, 584, A117
Neumann, W. O., Breuer, D., & Spohn, T. 2016a, LPSC, 47, 2307
Neumann, W. O., Breuer, D., & Spohn, T. 2016b, in AAS/Division for Planetary Sciences Meeting, 48, #506.08
Neveu, M., Desch, S. J., & Castillo-Rogez, J. C. 2015, JGRE, 120, 123
Pedersen, K. 2000, FEMS Microbiology Letters, 185, 9
Porco, C., Helfenstein, P., Thomas, P., et al. 2006, Sci, 311, 1393
Postberg, F., Kempf, S., Schmidt, J., et al. 2009, Natur, 459, 1098
Roberts, J. H. 2015, Icar, 258, 54
Roth, L., Saur, J., Retherford, K. D., et al. 2014, Sci, 343, 171
Sherwood Lollar, B., Onstott, T., Lacrampe-Couloume, G., & Ballentine, C. 2014, Natur, 516, 379
Sim, Y.-J., & Kim, H.-T. 2005, J. Korean Geotech. Soc., 21, 45
Sparks, W., Hand, K., McGrath, M., et al. 2016, ApJ, 829, 121
Spinks, J. W. T., & Woods, R. J. 1990, IAEA INIS, Vol. 22, Issue 15 (New York: Wiley)
Tarnas, J. D., Mustard, J. F., Sherwood Lollar, B., & Bramble, M. S. 2017, LPSC, 48, 2030
Thomas, P., Tajeddine, R., Tiscareno, M., et al. 2016, Icar, 264, 37
Vance, S., Hand, K., & Pappalardo, R. 2016, GeoRL, 43, 4871
Vance, S., Harnmeijer, J., Kimura, J., et al. 2007, AsBio, 7, 987
Waite, J. H., Glein, C. R., Perryman, R. S., et al. 2017, Sci, 356, 6334
Zheng, W., Jewitt, D., & Kaiser, R. I. 2006, ApJ, 639, 534
Zolotov, M. Y. 2009, Icar, 204, 183